Responses to Reviewers' Comments on Manuscript EGUSPHERE- 2024-1325

(Molecular and seasonal characteristics of organic vapors in urban Beijing: insights from Vocus-PTR measurements)

We have addressed each comment in the following paragraphs and made the corresponding changes in the revised manuscript. The reviewers' comments are shown in blue italic text, followed by our responses. Changes in the revised manuscript are highlighted and presented as "quoted underlined text" in our responses.

Reviewer #1:

Scientific significance:

In my opinion the significance of this paper is good. It shows the differences of VOC emissions for different seasons and also analyzes the influence of day and night times on VOC emissions.

Scientific quality:

The scientific quality is ok, however the errors of the measurements need to be included and better presented.

Presentation quality:

The presentation quality is good but can be improved by explaining what the influence of OSc and DBE is. And why it is important for this paper. It is explained in detail how it is calculated (which in my opinion can also be placed in the supporting material part) but the influence on the atmosphere is not made clear enough.

Response: We appreciate the comments. We have addressed the above general comments in detail in the following responses.

General comments:

First of all, you need to clarify the term concentration. This term isn't used correctly in the whole paper. A concentration is defined as mass/volume what you measured with you Vocus is a mixing ratio (in this case a volume mixing ratio). You correctly used the unit ppt/ppb. However, to further clarify that you are talking about volume mixing-ratios you can either say it once and than say you will use ppb/ppt as a unit of volume mixing ratios or you can use.

Response: The reviewer is correct. We have replaced the term "concentration" with "mixing ratio" throughout the manuscript.

Introduction

You don't need to include all the different PTRs. Here just make clear what the advantage is (higher sensitivity and lower detection limits), how it is achieved ("incorporating radio frequency electric fields to focus ions") and the disadvantage (lighter ions are cut off to protect the detector from overloading). Another disadvantage compared to GC and other methods is that you can't be sure on the exact compound. You only get the information of the exact mass and from this you get information on a sum formular. However, you don't know anything about the functional groups etc. (no chance to differentiate between ketones and aldehydes).

Response: Thanks for the suggestion. We have summarized the improvements in PTR and described them in one sentence. We also added their disadvantages, one being the cut off of lighter ions, and the other being the inability to distinguish the exact compound. The modifications in the main text are as follows:

[Line 78 to 85] Recent developments in the ion-molecule reactor (IMR) configuration have greatly increased sensitivities and concurrently lowered the limits of detection of PTR-MS by several orders of magnitude by incorporating radio frequency electric fields to focus ions (Breitenlechner et al., 2017; Krechmer et al., 2018; Reinecke et al., 2023). A consequential issue is that these advanced PTR-MS typically need to eliminate lighter ions to protect the detector from overload, and similar to traditional PTR-MS, they are incapable of obtaining molecular structure information.

Why are you only comparing data from PTR, if you want to see higher oxidized compounds people used other methods. (Iodide-CIMS, nitrate-CIMS…). However I don't know if studies were conducted with those techniques in the past in this way. If there were studies, just include some examples.

Response: Thanks for the suggestion. Yes, other CIMS (nitrate, iodide, bromide, and ammonium-CIMS) are usually used to study oxygenated organic molecules. We have included them in the Introduction. This paragraph in the main text is revised as follows:

[Line 86 to 101] These improvements have expanded the detection capabilities of PTR-MS, particularly for organic vapors with lower volatility and multiple oxygens (≥3) (Riva et al., 2019), which enables the simultaneous measurement of VOC precursors and their primary, secondary, and higher-level oxidation products using a single instrument (Li et al., 2020). Despite their low concentrations, these vapors may condense onto pre-existing aerosols and make a significant contribution to secondary aerosol growth and cloud condensation nuclei (Bianchi et al., 2019; Pospisilova et al., 2020; Nie et al., 2022). Organic vapors with multiple oxygens are likely to be simultaneously detected by other chemical ionization mass

spectrometry (CIMS), e.g., nitrate (NO_3^-), iodide (I^-), bromide (Br^-), and ammonium (NH_4^+) (Riva et al., 2019; Huang et al., 2021), which are widely used for measuring oxygenated organic compounds in the atmosphere (Bianchi et al., 2019; Ye et al., 2021; Huang et al., 2021). Therefore, using these improved PTR-MS can supplement our understanding of oxygenated organic vapors and facilitate the study of atmospheric chemical evolution of organics (Wang et al., 2020a).

2.1.

How do you account for fragments, you seem to use a quite hard setting. What is your E/N? I know it is hard to calculate but you can find some help in this publication: Jensen, A., Koss, A. R., Hales, R., and de Gouw, J. A.: Measurements of VOCs in ambient air by Vocus PTR-TOF-MS: calibrations, instrument background corrections, and introducing a PTR Data Toolkit, Atmos. Meas. Tech., 16, 5261–5285, doi:10.5194/amt-16-5261-2023, 2023.

Response: Thanks for the suggestion. The E/N in our study was 146.9 Td, which in case limited the formation of water clusters, promoted the simple reaction kinetics, but may lead to fragmentation. Here, we corrected the fragmentation, water cluster, and interferences for calibrated and uncalibrated species.

For α-pinene, we identified its fragments based on GC chromatograms. The Vocus-PTR was calibrated in GC mode before atmospheric observation. We tested a total of 4 species (shown in Figure R1a), including severely fragmented α-pinene. The spectrum of α-pinene is shown in the Figure R1b, with the main fragment being $C_6H_9^+$. We also investigated the potential interference of ion $C_{10}H_{19}O^+$. Since the correlation between $C_{10}H_{17}^+$ and $C_{10}H_{19}O^+$ was not strong ($0.33 < r < 0.72$) and the mixing ratio of $C_{10}H_{19}O^+$ was two orders of magnitude lower than $C_{10}H_{17}^+$, the impact of $C_{10}H_{19}O^+$ was not considered.

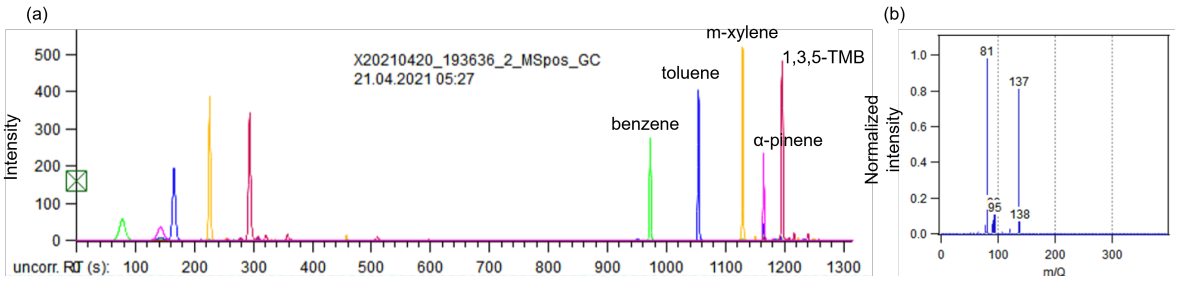

Figure R1. GC-Vocus results. (a) GC chromatogram of 4 species. (b) MS spectrum of α-pinene.

Several long-chain aldehydes and cycloalkanes may fragment on $C_5H_8H^+$, the ion typically attributed to isoprene in PTR-MS (Gueneron et al., 2015; Pfannerstill et al., 2023; Coggon et al., 2024). We corrected isoprene signals following an approach by Coggon et al. (2024). The correction is calculated as follows:

$$m/z\ 69.07_{Corrected} = S_{69.07} - S_{111.12+125.13} \cdot f_{69.07/(111.12+125.13)}$$

$S_{69.07}$ is the signal measured at $C_5H_9^+$. $S_{111.12+125.13}$ is the signal of the isoprene interferences, referring to $C_8H_{15}^+$ (m/z 111.12) and $C_9H_{17}^+$ (m/z 125.13), which are dehydrated products from octanal and nonanal, respectively. $f_{69.07/(111.12+125.13)}$ is determined from nighttime data (0:00-4:00) of each period. Similarly, acetaldehyde was corrected for ethanol fragments. We also checked the fragments and water cluster list in Pfannerstill et al. (2023) and Jensen et al. (2023). When the Pearson correlation coefficient r was greater than 0.95, we considered that the ions were fragments or water clusters of the parent ion.

We also tried to exclude the effects of unknown fragments and water clusters based on correlations of times series. Similar to Pfannerstill et al. (2023), any ion showing a correlation with another ion with $r^2 > 0.97$ (if chemical reasonable) was analyzed for possible water clustering or fragmentation effects and added up with its parent ion. The ions corrected are listed as follows: $C_2H_4N^+$ with water cluster $C_2H_6NO^+$, $C_3H_7O^+$ with water cluster $C_3H_9O_2^+$, $C_5H_9^+$ with fragment $C_5H_7^+$, $C_7H_9^+$ with fragment $C_7H_7^+$, CH_4NO^+ with water cluster $CH_6NO_2^+$, $C_2H_7O^+$ with water cluster $C_2H_9O_2^+$, $C_3H_3O_2^+$ with water cluster $C_3H_5O_3^+$, $C_4H_5O_2^+$ with water cluster $C_4H_7O_3^+$, $C_3H_5^+$ with fragment $C_3H_3^+$, $C_2H_5O^+$ with water cluster $C_2H_7O_2^+$, $C_2H_4NO^+$ with water cluster $C_2H_6NO_2^+$, $C_4H_5O_2^+$ with water cluster $C_4H_7O_3^+$, $C_3H_3O_3^+$ with water cluster $C_3H_5O_4^+$, $C_6H_6NO^+$ with water cluster $C_6H_8NO_2^+$, $C_8H_8NO_2^+$ with water cluster $C_8H_{10}NO_3^+$, $C_{10}H_{21}O^+$ with water cluster $C_{10}H_{23}O_2^+$, $C_9H_{13}O_3^+$ with water cluster $C_9H_{15}O_4^+$, $C_{10}H_{13}O_3^+$ with water cluster $C_{10}H_{15}O_4^+$, and $C_{14}H_{13}^+$ with water cluster $C_{14}H_{15}O^+$.

We acknowledge that this method cannot identify all fragments and clusters, and fragments and clusters may still be present in the measured VOCs and OVOCs. Further research is needed to explore the impact of fragments and clusters on the measurements, particularly concerning OVOCs with multiple oxygens.

We have added one paragraph in the main text to address the potential fragments and water clusters. See line 228 to 264 in the main text.

The fragmentation, water cluster, and interferences for calibrated and uncalibrated species were corrected. The ratio of the electric field strength (E) to the buffer gas number density (N) used in our study was 146.9 Td, and the gradient between BSQ skimmer 1 and skimmer 2 was 9.8 V, which in case limited the formation of water clusters, promoted the simple reaction kinetics, and improved the sensitivity, but may lead to stronger fragmentation. For α-pinene, we identified its fragments based on GC chromatograms. The Vocus-PTR was calibrated in GC mode before atmospheric measurement. A total of 4 species were tested in GC mode, including severely fragmented α-pinene. The spectrum of α-pinene showed that the main fragment was $C_6H_9^+$. Several long-chain aldehydes and cycloalkanes may fragment on $C_5H_8H^+$, the ion typically attributed to isoprene in PTR-MS (Gueneron et al., 2015; Pfannerstill et al., 2023a; Coggon et al., 2024). We corrected isoprene signals following an approach by Coggon et al. (2024). The correction was calculated as follows:

$$\text{m/z } 69.07_{\text{Corrected}} = S_{69.07} - S_{111.12+125.13} \cdot f_{69.07/(111.12+125.13)} \quad (1)$$

$S_{69.07}$ is the signal measured at $C_5H_9^+$. $S_{111.12+125.13}$ is the signal of the isoprene interferences, referring to $C_8H_{15}^+$ (m/z 111.12) and $C_9H_{17}^+$ (m/z 125.13), which are dehydrated products from octanal and nonanal, respectively. $f_{69.07/(111.12+125.13)}$ was determined from nighttime data (0:00-4:00) of each period. Similarly, acetaldehyde was corrected for ethanol fragments. We also checked the fragments and water cluster list in Pfannerstill et al. (2023a) and Jensen et al. (2023). When the Pearson correlation coefficient r is greater than 0.95, the ions were considered as fragments or water clusters of the parent ion. We also tried to exclude the effects of unknown fragments and water clusters based on correlations of times series. Similar to Pfannerstill et al. (2023a), any ion showing a correlation with another ion with $r^2 > 0.97$ (if chemical reasonable) was analyzed for possible water clustering or fragmentation effects and added up with its parent ion. The ions corrected are listed as follows: $C_2H_4N^+$ with water cluster $C_2H_6NO^+$, $C_3H_7O^+$ with water cluster $C_3H_9O_2^+$, $C_5H_9^+$ with fragment $C_5H_7^+$, $C_7H_9^+$ with fragment $C_7H_7^+$, CH_4NO^+ with water cluster $CH_6NO_2^+$, $C_2H_7O^+$ with water cluster $C_2H_9O_2^+$, $C_3H_3O_2^+$ with water cluster $C_3H_5O_3^+$, $C_4H_5O_2^+$ with water cluster $C_4H_7O_3^+$, $C_3H_5^+$ with fragment $C_3H_3^+$, $C_2H_5O^+$ with water cluster $C_2H_7O_2^+$, $C_2H_4NO^+$ with water cluster $C_2H_6NO_2^+$, $C_4H_5O_2^+$ with water cluster $C_4H_7O_3^+$, $C_3H_3O_3^+$ with water cluster $C_3H_5O_4^+$, $C_6H_6NO^+$ with water cluster $C_6H_8NO_2^+$, $C_8H_8NO_2^+$ with water cluster $C_8H_{10}NO_3^+$, $C_{10}H_{21}O^+$ with water cluster $C_{10}H_{23}O_2^+$, $C_9H_{13}O_3^+$ with water cluster $C_9H_{15}O_4^+$, $C_{10}H_{13}O_3^+$ with water cluster $C_{10}H_{15}O_4^+$, and $C_{14}H_{13}^+$ with water cluster $C_{14}H_{15}O^+$.

Was a heating installed around your inletline and was it kept constant? If not, this might also explain your observation of less IVOCs and SVOCs in winter times.

Response: The sampling tube was heated to 50 ± 5°C during the observation periods to lower the impacts on IVOCs and SVOCs. We have added this information in the main text.

Were the meteorological parameters somehow included in your analysis?

Response: We included the analysis of meteorological parameters into the analysis of diurnal variations across different clusters, and also made corresponding revisions in the main text.

[Line 488 to 495] Daytime clusters start to rise at 6:00-7:00 (6:00 for summer and 7:00 for other seasons), peak at 11:00-14:00 and then slowly decrease, following the diurnal variation of solar radiation (Li et al., 2023), ozone and temperature (Fig. S2). Figure S10 further demonstrates the dependence of daytime clusters on temperature. The mixing ratio of daytime clusters show an apparent increase in summer (when temperature is higher than 15 °C), which indicates that higher temperatures accompanied by an increase in solar radiation and ozone favors the formation of daytime clusters.

[Line 497 to 500] In summer, the vast majority of species (77%) exhibit daytime characteristics, with a mixing ratio percentage as high as 85%, which may be related to the strongest solar radiation (Li et al., 2023) and lowest NOx concentrations (Fig. S2).

[Line 504 to 505] The afternoon peak of daytime clusters in autumn and winter are accompanied by a decrease in mixing layer height (Li et al., 2023).

[Line 522 to 524] Nighttime clusters also show better consistency with $PM_{2.5}$ compared to daytime clusters (Fig. S2), which may be related to mixed sources.

2.2.

Your cut off is above the mentioned 35 amu. This needs to be told here. In the supplementary information the equations of linearity and transmission curve would also be a nice add on. Additionally, I don't like the idea of using the mean of those three compounds (supplementary). I understand that you had to exclude the others due to your transmission curve. However, the error will be too low compared to the error that is expected if you only have 3 compounds with which you actually had to get the linearity alone. It is not always true that the offset is "0" which you claimed to be true. If you had used a softer setting you might not be able to detect compounds with a low k-rate. Therefore, the offset might even be negative. This error could be minimized by using compounds with higher and lower k-rates. Here however, all compounds

had nearly the same k-rate. Luckily the k-rates were the k-rates that were by default anyhow used for most of the compounds. I would suggest to at least make this fit with those three compounds and if the error is high you need to show this.

Response: Thanks for the comments and suggestions. We have modified this part and describe it as follows:

Firstly, we used more compounds to determine the linearity. As mentioned in Table S2, we used 2 cylinders of calibration gas to calibrate the Vocus-PTR during different observation periods. Although the sensitivities of calibration gases varied across different observation periods, the relative sensitivities to toluene were comparable. We plot the sensitivities of the 2 cylinders of calibration gas together in Figure R2a. The y axis is the normalized sensitivity to toluene, and the x axis is their corresponding k_{PTR}. The black squares represent calibration gases from cylinder 1, and the black dots represents calibration gases from cylinder 2.

Then, we refitted the linearity using $C_7H_9^+$, $C_8H_{11}^+$, $C_9H_{13}^+$, $C_{10}H_9^+$, and $C_5H_9O_2^+$, with the result of the linear fit shown by the black line in the figure. The equation is y = 0.43x+0.23 with an R^2 of 0.87. Note that the sensitivity of toluene needs to be multiplied when using the equation. The offset is 0.23, not 0, which is also in accordance with the review's comment. The species with gray labels have lower sensitivities due to the influence of transmission, so it is necessary to correct for the transmission efficiency.

Thirdly, we calculated the transmission efficiency based on these calibration gases, as shown in Figure R2b. the cut off is around 40, we have added this information in the main text.

Lastly, we updated the whole measurement data using the new linearity and transmission efficiency.

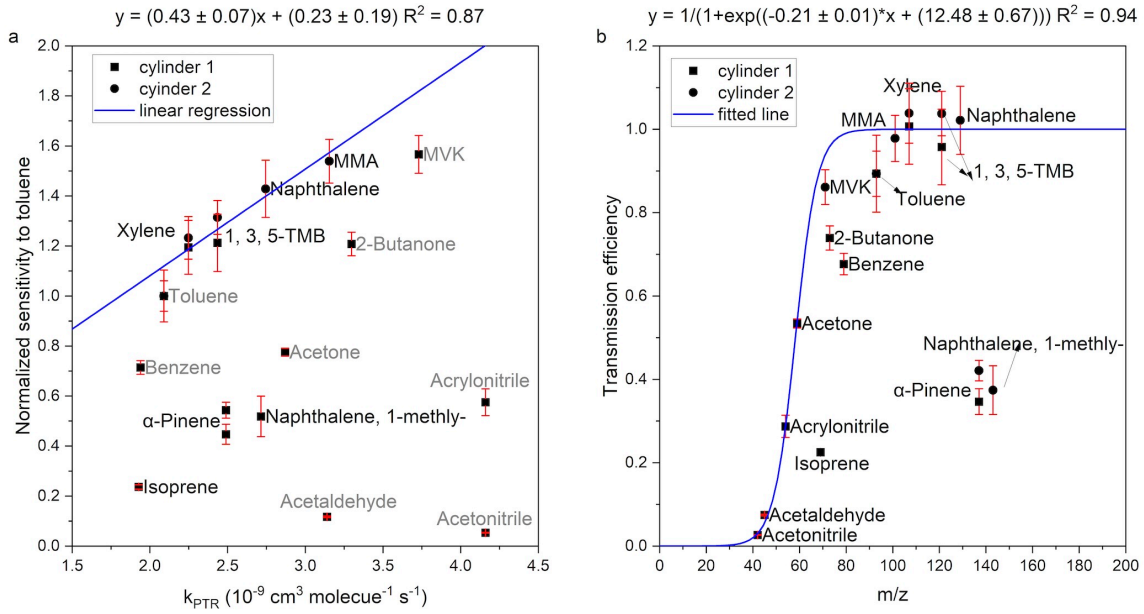

Figure R2 (also shown as Figure S3 in the supplementary). Calibration results of mixed calibration gases. (a) The scatter plot of the sensitivities of mixed calibration gases and their k_{PTR}. The blue line is the linear fitting of $C_7H_9^+$, $C_8H_{11}^+$, $C_9H_{13}^+$, $C_{10}H_9^+$, and $C_5H_9O_2^+$, respectively. The error bar refers to standard deviation. The sensitivities of species with gray labels are affected by transmission. (b) The transmission efficiency of mixed calibration gases. The blue line is the fitted transmission efficiency curve based on that of mixed calibration gases. The error bar refers to standard deviation.

We have also revised the main text:

[Line 200 to 216] Figure S3a shows the measured sensitivities of mixed calibration gases and their corresponding k_{PTR} values. The linear regression between kPTR and sensitivities was obtained based on sensitivities of $C_7H_9^+$, $C_8H_{11}^+$, $C_9H_{13}^+$, $C_{10}H_9^+$, and $C_5H_9O_2^+$ with an R^2 of 0.87. Sensitivities of other ions in mixed calibration gases may be influenced by transmission (ions labeled as gray) and fragmentation ($C_5H_9^+$, $C_{10}H_{17}^+$ and $C_{11}H_{11}^+$). The transmission efficiency of mixed calibration gases was calculated using sensitivities of mixed calibration gases, as shown in Figure S3b. The transmission efficiency of mixed calibration gases aligns well with the fitted transmission efficiency curve, except for $C_5H_9^+$, $C_{10}H_{17}^+$ and $C_{11}H_{11}^+$, which potentially experience fragmentation (fragmentation of measured ions are discussed below). For organic vapors without standards, their theoretical k_{PTR} were used to constrain sensitivities, while for organic vapors with no theoretical k_{PTR}, an average k_{PTR} of known species, 2.5×10-9 cm^3 $molecule^{-1}$ s^{-1} was used to constrain their sensitivities. The theoretical k_{PTR} of organic vapors are from previous studies (Zhao and Zhang, 2004; Cappellin et al., 2012; Sekimoto et al., 2017).

The fragmentation of C10H17+ would be nice to see, the most abundant fragment is C9H6+. (to have an idea on the fragmentation strength; however, this is only helpful not mandatory)

Response: Thanks for the suggestion. We have checked and corrected the fragments of $C_{10}H_{17}^+$ based on GC chromatograms, and the fragmentation ratio was 52.8 ± 10.6 for $C_{10}H_{17}^+$. We have added one paragraph in the main text to address the potential fragments and water clusters. Please refer to the response to the comment "*How do you account for fragments…*" and see line 228 to 264 in the main text.

Make clear why you use DBE and OSc. What do you expect and what does it say? If you answer this, your analysis part will be easier to understand.

Response: Thanks for the suggestion. DBE represents the degree of unsaturation. The DBE of organic vapor with multiple oxygens is influenced by oxidation process and its precursors (if has). For example, aromatic VOCs have DBE values no smaller than 4, while aliphatic VOCs usually have DBE values smaller than 2 (Nie et al., 2022). For organic vapors with DBE between 2-3, they are likely oxidation products of aliphatic and aromatic VOCs (Nie et al., 2022). We also compare the OSc for organic vapors with different oxygens. For the same number of carbon atoms, organic vapors with a higher number of oxygen atoms exhibit a higher carbon oxidation state, which indicates a functionalization process (Kroll et al., 2011). We have revised and added discussions on DBE and OSc in the main text, and we also moved the calculation methods of DBE, OSc, and volatility to the Supporting Information.

[Line 371 to 379] Aromatic VOCs have DBE values no smaller than 4, while aliphatic VOCs usually have DBE values smaller than 2. For organic vapors with DBE between 2-3, they are likely oxidation products of aliphatic and aromatic VOCs (Wang et al., 2021b; Nie et al., 2022). For the same number of carbon atoms, organic vapors with a higher number of oxygen atoms exhibit a higher carbon oxidation state (as shown in Figure S5). Compared to organic vapors with 3 or 4 oxygen atoms, organic vapors with 5 or more oxygens have undergone more extensive atmospheric oxidation and functionalization processes (Kroll et al., 2011; Isaacman-Vanwertz et al., 2018).

Line 220: there is an additional box in the text

Response: Revised.

Paragraph 328 ff

Isoprene is a bad example when ozone is present. In (https://amt.copernicus.org/articles/16/1179/2023/amt-16-1179-2023.pdf) it is described that oxidized compounds can fragment in the ion source of a PTR (also Vocus) and land on the exact mass as isoprene does. Therefore, the isoprene signal can be overestimated.

Response: We have corrected isoprene signals following an approach by Coggon et al. (2024). We have added one paragraph in the main text to address the potential fragments and water clusters. Please refer to the response to the comment "*How do you account for fragments…*" and see line 228 to 264 in the main text.

Paragraph 355 ff

Cold inlet line might also explain lower SVOC mixing ratios

Response: Thanks for the reminder. The sampling tube was heated to 50 ± 5℃ during the observation periods to lower the impacts on IVOCs and SVOCs.

"Day time cluster"

Do I understand correctly, all VOCs increase at 6 am? There should be seasonal changes (due to changing light conditions), or is there another source (e.g. traffic, factories?)

Response: We appreciate the reviewer's suggestions. After carefully comparing the diurnal variations across different seasons, we found that in spring, autumn, and winter, the daytime clusters start to increase after 7:00 AM, whereas in summer, the increase begins after 6:00 AM. Another seasonal change is that the number and corresponding mixing ratios of species allocated to the daytime clusters vary in four seasons. In summer, the vast majority of species (77%) exhibit daytime characteristics, with a mixing ratio percentage as high as 85%, which may be related to the strongest solar radiation and lowest NOx concentrations. We also made revisions in the main text.

[Line 488 to 505] Daytime clusters start to rise at 6:00-7:00 (6:00 for summer and 7:00 for other seasons), peak at 11:00-14:00 and then slowly decrease, following the diurnal variation of solar radiation (Li et al., 2023), ozone and temperature (Fig. S2). Figure S10 further demonstrates the dependence of daytime clusters on temperature. The mixing ratio of daytime clusters show an apparent increase in summer (when temperature is higher than 15 °C), which indicates that higher temperatures accompanied by an increase in solar radiation and ozone favors the formation of daytime clusters. The number and corresponding mixing ratios of species allocated to the daytime clusters vary in four seasons. In summer, the vast majority of species (77%) exhibit daytime characteristics, with a mixing ratio percentage as high as 85%, which may be related to the strongest solar radiation (Li et al., 2023) and lowest NOx concentrations (Fig. S2). The contribution of daytime clusters in autumn is also significant, with 67% and 58% of the species and mixing ratios being accounted for. The noon peaks of daytime clusters in winter and spring are relatively less pronounced, with the species and mixing ratio day/night ratios also being comparatively lower. The afternoon peak of daytime clusters in autumn and winter are accompanied by a decrease in mixing layer height (Li et al., 2023).

Is it possible to check for inversion layer and/or boundary layer. Especially, in winter this can decrease the efficiency of dilution. (meteorological data)

Response: Thanks for the suggestion. Unfortunately, we did not measure boundary layer height. However, we checked and referenced the MLH data in Li et al. (2023) between December 2019 to August 2021 measured by a ceilometer. The sampling site in Li et al. (2023) was on the fifth floor of a building on the west campus of Beijing University of Chemical Technology, approximately 6.5 km away from our site. This MLH data covered the spring and summer time of our sampling period. We compared the other parameters measured in Li et al. with those in our study. Although the absolute values differ, the relative seasonal trends are consistent. We included MLH analysis in the main text.

[Line 477 to 478] The seasonal variations of OVOCs are partly caused by the variation of mixing layer height (Li et al., 2023), which is lowest in winter.

[Line 504 to 505] The afternoon peak of daytime clusters in autumn and winter are accompanied by a decrease in mixing layer height (Li et al., 2023).

Line 457 style no "the" in front of winter

Response: Revised.

Line 459 style better: in winter in Beijing during the last few years

Response: Revised.

Line 466 just keep in mind that there will be fragments on the isoprene mass…

Response: We have corrected isoprene signals following an approach by Coggon et al. (2024). We have added one paragraph in the main text to address the potential fragments and water clusters. Please refer to the response to the comment "*How do you account for fragments…*" and see line 228 to 264 in the main text.

Supporting information

Figure S3 as mentioned above the compounds C8H11+, C9H13+ and C7H9+ would be needed to fit the k-rate to sensitivity line and not just the mean of all three slopes.

Response: We have modified the method for determining the sensitivity. Please refer to the response to the comment "*Your cut off is above the mentioned 35 amu.…*" and see line 200 to 216 in the main text.

Figure S9 Which vmr is plotted here? The sum of all? What does this graph say? You see less when it's cold? (explain your figure in a few sentences)

Response: The vmr plotted here is the sum of daytime clusters. The mixing ratio of daytime clusters show an apparent increase in summer (when temperature is higher than 15 Degree Celsius), which indicates that higher temperatures accompanied by an increase in solar radiation (Li et al., 2023) favors the formation of daytime clusters. We revised the figure caption and the main text.

[Line 492 to 495] The mixing ratio of daytime clusters show an apparent increase in summer (when temperature is higher than 15 °C), which indicates that higher temperatures accompanied by an increase in solar radiation and ozone favors the formation of daytime clusters.

Figure S10 Which vmr is plotted against which? I assume it's sum of nighttime cluster (x-axis) against sum of CxHyO1-2 compounds?

Response: It's the sum of nighttime clusters (x-axis) against the sum of the cluster 1 of CxHyO1-2 compounds. We have revised the caption.

Table S2 under the table a "Benzene" is missing (1,3,-dichloro-) no "," between 1,1-dichloro- and benzene (1,1-dichloro-benzene). Why are those compounds not included? They are quite heavy and it would definitively help to get a better idea on your k-rate to sensitivity plot and also in your transmission curve plot.

Response: Thanks for the reminder. We tested some chlorine-containing compounds in the lab before the observation started, but our Vocus had very low sensitivity to these chlorine-containing compounds (as shown in Figure R3). Therefore, we did not include these compounds in the subsequent data processing. We also deleted this sentence to avoid misunderstanding and all species are used for instrument calibration in the revised table.

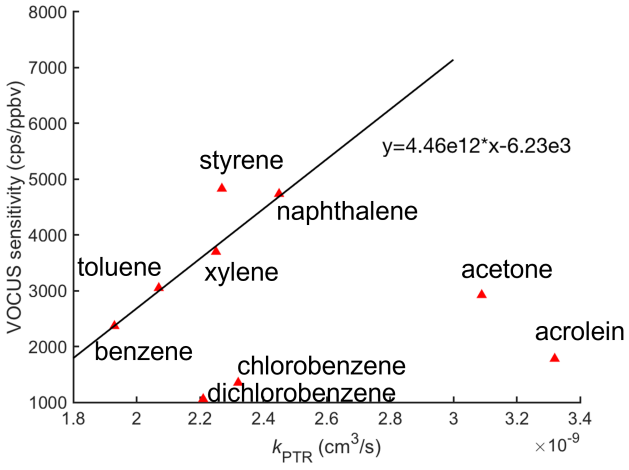

Figure R3. Sensitivities for chlorine-containing compounds and other compounds.

References:

Coggon, M. M., Stockwell, C. E., Claflin, M. S., Pfannerstill, E. Y., Xu, L., Gilman, J. B., Marcantonio, J., Cao, C., Bates, K., Gkatzelis, G. I., Lamplugh, A., Katz, E. F., Arata, C., Apel, E. C., Hornbrook, R. S., Piel, F., Majluf, F., Blake, D. R., Wisthaler, A., Canagaratna, M., Lerner, B. M., Goldstein, A. H., Mak, J. E., and Warneke, C.: Identifying and correcting interferences to PTR-ToF-MS measurements of isoprene and other urban volatile organic compounds, Atmos. Meas. Tech., 17, 801-825, 10.5194/amt-17-801-2024, 2024.

Gueneron, M., Erickson, M. H., VanderSchelden, G. S., and Jobson, B. T.: PTR-MS fragmentation patterns of gasoline hydrocarbons, Int. J. Mass Spectrom., 379, 97-109, 10.1016/j.ijms.2015.01.001, 2015.

Jensen, A. R., Koss, A. R., Hales, R. B., and de Gouw, J. A.: Measurements of volatile organic compounds in ambient air by gas-chromatography and real-time Vocus PTR-TOF-MS: calibrations, instrument background corrections, and introducing a PTR Data Toolkit, Atmos. Meas. Tech., 16, 5261-5285, 10.5194/amt-16-5261-2023, 2023.

Kroll, J. H., Donahue, N. M., Jimenez, J. L., Kessler, S. H., Canagaratna, M. R., Wilson, K. R., Altieri, K. E., Mazzoleni, L. R., Wozniak, A. S., Bluhm, H., Mysak, E. R., Smith, J. D., Kolb, C. E., and Worsnop, D. R.: Carbon oxidation state as a metric for describing the chemistry of atmospheric organic aerosol, Nature Chemistry, 3, 133-139, 10.1038/nchem.948, 2011.

Li, X., Chen, Y., Li, Y., Cai, R., Li, Y., Deng, C., Wu, J., Yan, C., Cheng, H., Liu, Y., Kulmala, M., Hao, J., Smith, J. N., and Jiang, J.: Seasonal variations in composition and sources of atmospheric ultrafine particles in urban Beijing based on near-continuous measurements, Atmos. Chem. Phys., 23, 14801-14812, 10.5194/acp-23-14801-2023, 2023.

Nie, W., Yan, C., Huang, D. D., Wang, Z., Liu, Y., Qiao, X., Guo, Y., Tian, L., Zheng, P., Xu, Z., Li, Y., Xu, Z., Qi, X., Sun, P., Wang, J., Zheng, F., Li, X., Yin, R., Dallenbach, K. R., Bianchi, F., Petäjä, T., Zhang, Y., Wang, M., Schervish, M., Wang, S., Qiao, L., Wang, Q., Zhou, M., Wang, H., Yu, C., Yao, D., Guo, H., Ye, P., Lee, S., Li, Y. J., Liu, Y., Chi, X., Kerminen, V.-M., Ehn, M., Donahue, N. M., Wang, T., Huang, C., Kulmala, M., Worsnop, D., Jiang, J., and Ding, A.: Secondary organic aerosol formed by condensing anthropogenic vapours over China's megacities, Nature Geoscience, 15, 255-261, 10.1038/s41561-022-00922-5, 2022.

Pfannerstill, E. Y., Arata, C., Zhu, Q., Schulze, B. C., Woods, R., Seinfeld, J. H., Bucholtz, A., Cohen, R. C., and Goldstein, A. H.: Volatile organic compound fluxes in the agricultural San Joaquin Valley – spatial distribution, source attribution, and inventory comparison, Atmos. Chem. Phys., 23, 12753-12780, 10.5194/acp-23-12753-2023, 2023.